



# Powder neutron diffraction studies for the $L2_1$ phase of $\text{Co}_2\text{YGa}$ ( $Y = \text{Ti, V, Cr, Mn}$ and $\text{Fe}$ ) Heusler alloys

R.Y. Umetsu<sup>a,\*</sup>, K. Kobayashi<sup>b,1</sup>, R. Kainuma<sup>a</sup>, Y. Yamaguchi<sup>c</sup>, K. Ohoyama<sup>c</sup>, A. Sakuma<sup>d</sup>, K. Ishida<sup>b</sup>

<sup>a</sup> Institute of Multidisciplinary Research for Advanced Materials, Tohoku University, 2-1-1 Katahira, Sendai 980-8577, Japan

<sup>b</sup> Department of Materials Science, Graduate School of Engineering, Tohoku University, 6-6-02 Aoba-yama, Sendai 980-8579, Japan

<sup>c</sup> Institute for Material Research, Tohoku University, 2-1-1 Katahira, Sendai 980-8577, Japan

<sup>d</sup> Department of Applied Physics, Graduate School of Engineering, Tohoku University, 6-6-05 Aoba-yama, Sendai 980-8579, Japan

## ARTICLE INFO

### Article history:

Received 10 February 2010

Received in revised form 19 February 2010

Accepted 26 February 2010

Available online 6 March 2010

### Keywords:

Co-based Heusler alloys

Degree of long range order

$L2_1$  phase

Magnetic moment

Neutron powder diffraction

## ABSTRACT

Site occupancies of Co, Y ( $Y = \text{Ti, V, Cr, Mn}$  and  $\text{Fe}$ ) and Ga atoms for the  $L2_1$  phase in  $\text{Co}_2\text{YGa}$  alloys annealed at 773 K were precisely investigated by powder neutron diffraction measurement. While Co atoms in all the five alloys almost perfectly occupy the  $x(2a)$  site, the occupancy of the  $z(4b)$  site by Ga atoms depends on the kind of Y atom, and it decreases with increasing number of valence electrons except for  $\text{Co}_2\text{CrGa}$  alloy. Degrees of long-range order on the  $z$  site occupancy of Ga atoms experimentally determined for all the alloys are in good agreement with those thermodynamically estimated from their order–disorder transition temperatures using the Bragg–Williams–Gorsky approximation.

© 2010 Elsevier B.V. All rights reserved.

## 1. Introduction

Half-metallic ferromagnets (HMFs) with a high spin polarization,  $P$  have been investigated intensively in the field of spintronics because magnetic tunnel junctions (MTJs) or current-perpendicular-to-plane (CPP) type spin valves consisting of HMFs are expected to have a huge tunnel magneto-resistance (TMR) or a giant magneto-resistance (GMR) [1–4]. Furthermore, HMFs are expected to be good candidates as ferromagnetic materials in spin-filter devices [5,6]. From theoretical calculations, it has been pointed out by de Groot et al. that the value of  $P$  in  $\text{NiMnSb}$  and  $\text{PtMnSb}$  alloys with the  $\text{C1}_b$  (half-Heusler)-type structure is perfect, namely,  $P = 100\%$  [7]. Kübler et al. have also pointed out that the density of state (DOS) in the minority spin state at the Fermi energy ( $E_F$ ) vanishes in  $\text{Co}_2\text{MnAl}$  and  $\text{Co}_2\text{MnSn}$  Heusler alloys [8]. Subsequently, electronic structures and high values of  $P$  for various  $L2_1$  (full-Heusler)-type alloys, such as  $\text{Co}_2\text{MnSi}$  and  $\text{Co}_2\text{MnGe}$ , have been calculated [9–12]. Recently, theoretical investigations have pointed out that the degree of long-range order for the Co-based  $L2_1$  phase ( $\text{Co}_2\text{YZ}$ ) is closely related to magnetic properties and  $P$ . For

example, Co-Y-type disordering significantly influences the magnetic properties [13–15] although Y-Z-type disordering does not affect those properties so much.

Our group has systematically investigated the  $L2_1$ -phase stability for the various Co-based Heusler alloys because phase stability is also one of the most important factors for the materials applicable to spintronics devices [15–19]. Fig. 1 indicates the order–disorder transformation temperatures from the  $L2_1$  to the  $B2$  phase,  $T_t^{L2_1/B2}$ , and Curie temperatures,  $T_C$ , for the  $L2_1$  phase in  $\text{Co}_2\text{YGa}$  ( $Y = \text{Ti, V, Cr, Mn}$  and  $\text{Fe}$ ) alloys [19]. Here, while being directly determined from the differential scanning calorimetric measurements for  $\text{Co}_2\text{CrGa}$ ,  $\text{Co}_2\text{MnGa}$  and  $\text{Co}_2\text{FeGa}$ , for the rest, the  $T_t^{L2_1/B2}$  was estimated by extrapolation from the experimental data for non-stoichiometric alloys because the  $T_t^{L2_1/B2}$  of  $\text{Co}_2\text{TiGa}$  and that of  $\text{Co}_2\text{VGa}$  alloys are higher than their melting points [18,19]. In this figure,  $T_t^{L2_1/B2}$  tends to decrease with an increasing number of valence electrons, except in the case of the  $\text{Co}_2\text{CrGa}$  alloy whose  $T_t^{L2_1/B2}$  is the lowest of the five alloys. Thermodynamic stability of the  $L2_1$  ordered phase can be discussed with  $T_t^{L2_1/B2}$ , because the alloy with a high  $T_t^{L2_1/B2}$  is presumed to have a high degree of order of the  $L2_1$  structure at room temperature or at the temperatures practically important for its use or fabrication process. However, determination of the degree of order for the  $L2_1$  phase in the  $\text{Co}_2\text{YGa}$  Heusler alloys using conventional powder X-ray diffraction is not easy because elements located in the same period of the periodic table show values of atomic scattering factor close to one another. On the other

\* Corresponding author. Tel.: +81 22 217 5816; fax: +81 22 217 5828.

E-mail address: [rie@tagen.tohoku.ac.jp](mailto:rie@tagen.tohoku.ac.jp) (R.Y. Umetsu).

<sup>1</sup> Present address: Technical Division, School of Engineering, Tohoku University, 6-6-11 Aoba-yama, Sendai 980-8579, Japan.

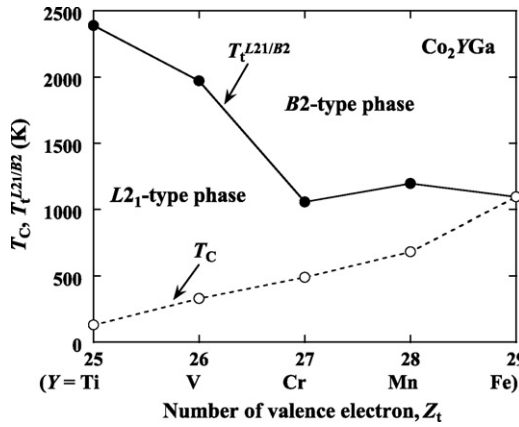


**Fig. 1.** Order–disorder transformation temperature from the  $L2_1$  to the  $B2$  phase  $T_t^{L21/B2}$  and the Curie temperature  $T_C$  for the  $L2_1$  phase in  $\text{Co}_2\text{YGa}$  ( $Y = \text{Ti}, \text{V}, \text{Cr}, \text{Mn}$  and  $\text{Fe}$ ) alloys [19].

hand, neutron diffraction (ND) has an advantage for examination of atomic ordering since the neutron scattering which occurs for atomic nucleus is basically independent of order in the periodic table. There have been many studies on various Co-based Heusler alloys except  $\text{Co}_2\text{CrGa}$  alloy using ND. For instance, investigations using powder ND have been performed for  $\text{Co}_2\text{TiGa}$  [20],  $\text{Co}_2\text{VGa}$  [21] and  $\text{Co}_2\text{MnGa}$  [22] alloys, and polarized ND for single crystals has been studied for  $\text{Co}_2\text{MnGa}$  and  $\text{Co}_2\text{FeGa}$  alloys by Brown et al. [23]. The ND examinations for the Co-based Heusler alloys reported in these literatures, however, have focused on the magnetic properties, and no systematic study on degree of long-range order of the Heusler structure has been performed. In the present study, degrees of long-range order of the  $L2_1$  structure in the  $\text{Co}_2\text{YGa}$  ( $Y = \text{Ti}, \text{V}, \text{Cr}, \text{Mn}$  and  $\text{Fe}$ ) Heusler alloys obtained in the same annealing conditions were systematically investigated using powder ND in a wide temperature range from 35 to 650 K, basically including both the ferromagnetic and the paramagnetic states. Correspondence between the estimated degree of long-range order and the reported order–disorder transition temperature for the  $\text{Co}_2\text{YGa}$  alloys was also evaluated with a thermodynamic consideration.

## 2. Experimental procedures

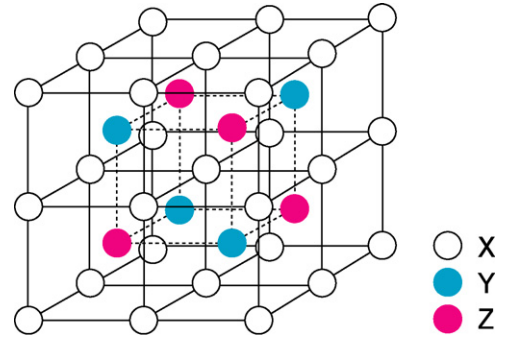
Five Heusler alloys of  $\text{Co}_2\text{YGa}$  ( $Y = \text{Ti}, \text{V}, \text{Cr}, \text{Mn}$  and  $\text{Fe}$ ) were fabricated by levitation melting and conventional induction melting under an argon atmosphere, respectively. The obtained ingots were annealed at 1373 or 1473 K for three days, followed by quenching in ice water. The microstructure of the annealed specimens was checked by an optical microscope, and alloy composition was evaluated by an electron probe microanalyzer (EPMA), where deviation from the nominal composition was confirmed to be less than 1 at.% for every element. The powder samples grained from the annealed bulk specimens were finally annealed at 773 K for 1 h in order to remove the slip defects and to heighten the degree of order of the  $L2_1$  structure. Powder ND measurements with high efficiency and resolution were carried out at temperatures ranging from 35 to 650 K with HERMES of the Institute for Materials Research (IMR), Tohoku University installed at the JRR-3M reactor in Japan Atomic Energy Agency (JAEA), Tokai, where neutrons with wave length of 0.18265 nm obtained by  $\{3\ 3\ 1\}$  reflection of a Ge monochromator were utilized. Fitting analyses for the experimental ND data were performed using the software “RIETAN-2000” [24] under the assumption that the alloy composition for every specimen is stoichiometric, where the refined parameters were within from 1.2 to 1.5 in the present refinement [24].

Fig. 2 shows the  $L2_1$ -type structure of  $X_2YZ$  Heusler alloy which is regarded as a structure consisting of eight bcc unit cells. Corner positions of the bcc unit cells (8c: x site) are occupied by X atoms and eight body-centered positions are alternately occupied by Y atoms (4a: y site) and Z atoms (4b: z site).

For ternary  $X_2YZ$ -type Heusler alloy with three sublattices, x, y and z, the atomic fraction of i atom occupying j site,  $f_i^j$ , is perfectly expressed with nine quantities which connect with the following six equations [26–29]:

$$f_x^x + f_x^y + f_x^z = f_y^x + f_y^y + f_y^z = f_z^x + f_z^y + f_z^z = 1, \quad (1)$$

$$f_x^x f_x + f_y^x f_y + f_z^x f_z = c_x, \quad f_x^y f_x + f_y^y f_y + f_z^y f_z = c_y, \quad f_x^z f_x + f_y^z f_y + f_z^z f_z = c_z, \quad (2)$$



**Fig. 2.** Structure of the  $L2_1$ -phase of the  $\text{Co}_2\text{YZ}$  Heusler alloy.

where  $c_i$  is the atomic fraction of element  $i$ ,  $f_i$  is the fraction of site  $i$  and  $f_x = 0.5$ ,  $f_y = 0.25$  and  $f_z = 0.25$  in the present case. Since the last equation of Eq. (2) is preceded by Eq. (1) and the remaining two equations of Eq. (2) and the number of relations is five, four quantities among the nine quantities are independent. This means that, in order to perfectly express the atomic configuration of the Heusler structure, four ordered parameters are required. The quantities,  $f_x^x$ ,  $f_z^z$ ,  $f_x^z$  and  $f_z^x$ , are selected as independent variables and then ordered parameters,  $S_1$ ,  $S_2$ ,  $S_3$  and  $S_4$ , are defined, respectively, by

$$S_1 = \frac{f_x^x - f_x}{1 - f_x} = 2f_x^x - 1, \quad S_2 = \frac{f_z^z - f_z}{1 - f_z} = \frac{4f_z^z - 1}{3},$$

$$S_3 = \frac{f_x - f_z}{f_x} = 1 - 4f_z^z, \quad S_4 = \frac{f_z - f_x}{f_z} = 1 - 2f_z^x. \quad (3)$$

For an alloy with a stoichiometric composition, namely,  $c_x = 0.5$ ,  $c_y = 0.25$  and  $c_z = 0.25$ , in the case of a perfectly ordered state,  $f_x^x = f_z^z = 1$  and  $f_x^z = f_z^x = 0$  and then  $S_1 = S_2 = S_3 = S_4 = 1$ , while in the case of disordered state,  $A2$  state  $f_x^x = f_z^z = 0.5$  and  $f_x^z = f_z^x = 0.25$ , and then  $S_1 = S_2 = S_3 = S_4 = 0$ . In the intermediate state of atomic arrangement, the  $S$  takes some values between zero and unity. For example, in the  $B2$  phase where the x sites are perfectly occupied by X atoms,  $f_x^x = 1$ ,  $f_z^z = 0.5$  and  $f_x^z = f_z^x = 0$ , and then  $S_1 = S_3 = S_4 = 1$  and  $S_2 = 1/3$ .

For the Heusler phase, because conventional diffraction examination gives only two kinds of relations on the site occupancy obtained from intensities of the  $\{1\ 1\ 1\}$ -type and the  $\{2\ 0\ 0\}$ -type superlattice reflections, two of the four order parameters are still independent. This means that no one can experimentally determine the atomic configuration for a Heusler phase only using the ND. Recently, the order–disorder transformation temperature from the  $B2$  to  $A2$  phase in the binary  $\text{CoGa}$  alloy was evaluated as being about 2550 K [25]. This suggests that at the annealing temperature of 773 K in the present study, it is difficult for the Co and Ga atoms to swap atomic sites with each other and that the  $f_z^{\text{Co}}$  and  $f_x^{\text{Ga}}$  can be approximately zero. Therefore,  $f_z^{\text{Co}} = f_x^{\text{Ga}} = 0$ , i.e.,  $S_3 = S_4 = 1$ , have been assumed in the present analysis. Under this assumption, the  $S_1$  and  $S_2$  in Eq. (3), which are the rest of the independent variables, are determined by the ND examination, and the atomic configuration of the Heusler structure can be perfectly estimated. Thus, the  $\varphi_1 \equiv S_1$  and  $\varphi_2 \equiv S_2$  are defined as long-range order parameters:

$$\varphi_1 = 2f_x^{\text{Co}} - 1, \quad (4)$$

$$\varphi_2 = \frac{1}{3}(4f_z^{\text{Ga}} - 1), \quad (5)$$

where the  $\varphi_1$  is actually the order parameter between Co and Mn atoms in the first nearest neighbors and the  $\varphi_2$  is mainly that between Ga and Mn in the second nearest neighbors.

## 3. Experimental results

### 3.1. $\text{Co}_2\text{TiGa}$

Fig. 3(a) and (b) shows the powder ND patterns at 300 and 35 K taken from  $\text{Co}_2\text{TiGa}$  alloy, respectively, where the experimental data and the calculated fitting curves are indicated by dots and solid red lines, respectively, and the blue lines at the bottom show the difference between them. Since the Curie temperature  $T_C$  of the  $\text{Co}_2\text{TiGa}$  alloy has been reported to be about 130 K [20,30,31], the profiles of (a) and (b) are in a paramagnetic and a ferromagnetic state, respectively. From the fitting analysis for the experimental ND obtained at 300 K in the paramagnetic region, the site occupancies  $f_x^{\text{Co}}$  and  $f_z^{\text{Ga}}$  are estimated to be 0.98 and 0.99, respectively, suggesting that the  $\text{Co}_2\text{TiGa}$  alloy exhibits an almost perfect degree

**Table 1**

The site occupancies of Co and Ga atoms on  $x$  and  $z$  sites,  $f_x^{\text{Co}}$  and  $f_z^{\text{Ga}}$ , respectively, for  $\text{Co}_2\text{YGa}$  ( $Y = \text{Ti, V, Cr, Mn and Fe}$ ) Heusler alloys, the lattice constant (nm), order–disorder transition temperature from the  $L_{21}$  to the  $B2$  phase  $T_{L_{21}/B2}^{\text{L}}$  (K), and the Curie temperature  $T_C$  (K) of the  $L_{21}$  phase in  $\text{Co}_2\text{YGa}$  alloys.  $\varphi_1^{\text{exp}}$  and  $\varphi_2^{\text{exp}}$  are obtained from  $f_x^{\text{Co}}$  and  $f_z^{\text{Ga}}$  with Eqs. (4) and (5), respectively, and  $\varphi_2^{\text{BWG}}$  is the degree of long-range order parameter evaluated by the Bragg–Williams–Gorsky approximation with Eq. (11) [26–29].

Y atom in $\text{Co}_2\text{YGa}$	Lattice constant (nm)	Occupancy		$T_{L_{21}/B2}^{\text{L}}$ (K)	$T_C$ (K)	$\varphi_1^{\text{exp}}$ at 35 K	$\varphi_2^{\text{exp}}$ at 35 K	$\varphi_2^{\text{BWG}}$
		$f_x^{\text{Co}}$	$f_z^{\text{Ga}}$					
Ti	0.5858 (at 300 K) 0.5837 (at 35 K)	0.98 0.99	0.990.99	2390	128	0.97	0.99	1.00
V	0.5781 (at 300 K) 0.5769 (at 35 K)	0.99 <sup>a</sup> 0.99 <sup>a</sup>	0.990.99	1970	341	0.96	0.99	0.99
Cr	0.5793 (at 573 K) 0.5741 (at 35 K)	0.99 0.98	0.900.88	1050	495	0.97	0.84	0.86
Mn	0.5803 (at 650 K) 0.5746 (at 35 K)	0.99 0.98	0.940.93	1195	685	0.98	0.91	0.92
Fe	0.5725 (at 35 K)	0.99	0.92	1093	1093	0.97	0.89	0.88

<sup>a</sup> The site occupancy  $f_x^{\text{Co}}$  is fixed as 0.99 for  $\text{Co}_2\text{VGa}$  alloy.

of order as the  $L_{21}$  phase. The site occupancies determined from the pattern at 35 K in the ferromagnetic region with the effect of magnetic scattering being taken into account are almost the same as those at 300 K as listed in Table 1. Since the atomic shift parameter strongly affects both the site occupancy and the magnetic scattering, we first evaluated the shift parameter using some peaks located at higher angles ( $2\theta > 80^\circ$ ) and then analyzed the site occupancy and the magnetic moments under fixed shift parameter. The magnetic moments estimated for Co and Ti atoms are about 0.38 and  $-0.08\mu_B/\text{atom}$ , respectively, being consistent with theoretical data [32] (0.59 and  $-0.08\mu_B/\text{atom}$ ) calculated with the linear muffin-tin orbital atomic sphere approximation (LMTO-ASA), respectively, and the reported experimental results obtained by ND ( $0.40\mu_B/\text{atom}$  for Co atom) [20,32]. All of the present numerical results for the lattice constant  $a$  (nm) and the occupancy of the Co and Ga atoms on the  $x$  and  $z$  sites, the degree of long-range order parameter  $\varphi_1^{\text{exp}}$ ,  $\varphi_2^{\text{exp}}$  being defined from Eqs. (4) and (5), long-range

order parameter evaluated by the Bragg–Williams–Gorsky approximation,  $\varphi_2^{\text{BWG}}$  and magnetic moments are listed in Tables 1 and 2, together with the theoretical and the experimental data on the magnetic moment reported in the previous papers.

### 3.2. $\text{Co}_2\text{VGa}$

Fig. 4(a) and (b) shows the powder ND patterns at 300 and 35 K taken from  $\text{Co}_2\text{VGa}$  alloy, respectively. Although the measured temperature  $T_m$  ( $=300$  K) for the pattern of Fig. 4(a) is lower than the  $T_C$  ( $=342$  K) [18,21], the contribution of the magnetic scattering was neglected in the analysis because the temperature difference was slight. Because the neutron scattering length of vanadium is almost zero, one more constrained condition should be added to determine the atomic configuration. The fitting analysis was performed under the assumption that the  $f_x^{\text{Co}}$  is 0.99 as well as the other alloys in the present study. As listed in Table 1, it was determined that  $f_z^{\text{Ga}} = 0.99$  and that the lattice constants at 300 and

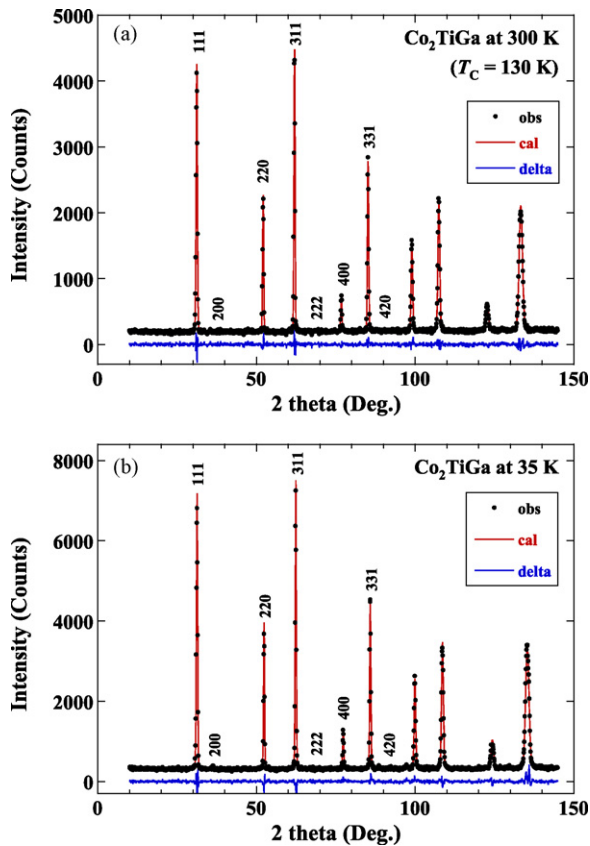


**Fig. 3.** Neutron powder diffraction patterns of  $\text{Co}_2\text{TiGa}$  alloy measured at 300 K (a) and at 35 K (b). The points are the observed counts and the solid lines the calculated one. The line at the bottom represents the difference between the observed and the calculated patterns.

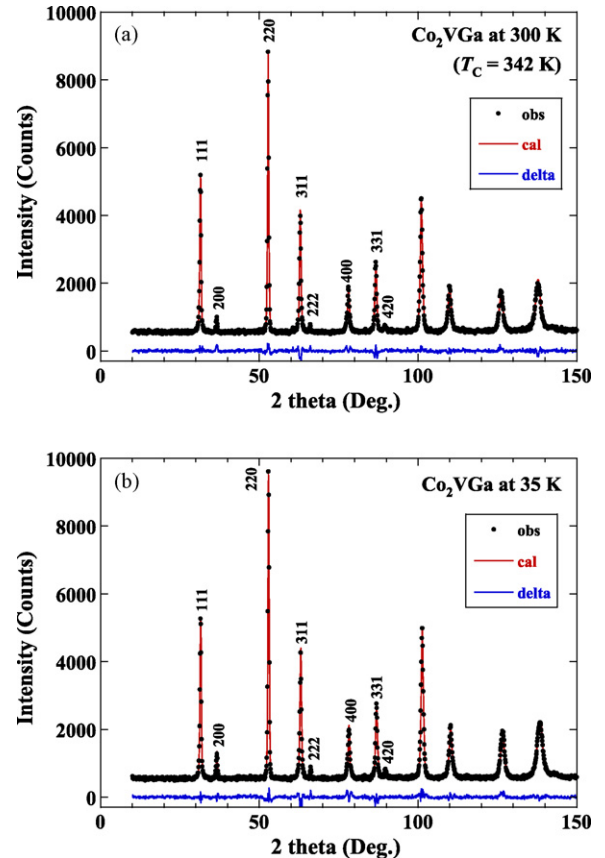


**Fig. 4.** Neutron powder diffraction patterns of  $\text{Co}_2\text{VGa}$  alloy measured at 300 K (a) and at 35 K (b), displayed in the same way as in Fig. 3.

**Table 2**

The magnetic moments of Co and Y (Y = Ti, V, Cr, Mn and Fe) obtained from the present neutron diffraction measurements at 35 K for Co<sub>2</sub>YGa alloys,  $m^{\text{exp}}$  and reported experimental results from neutron diffractions  $m^{\text{exp[Ref.]}}$ , together with the theoretically calculated values taken from the literature,  $m^{\text{cal}}$ , and total magnetic moment  $M$  ( $\mu_B/\text{f.u.}$ ). Magnetic moments of Cr, Mn and Fe on the z site are also listed in parentheses.

		Magnetic moment, $m$ ( $\mu_B$ )			Total magnetic moment, $M$ ( $\mu_B/\text{f.u.}$ )		
		$m^{\text{exp}}$	$m^{\text{exp[Ref.]}}$	$m^{\text{cal[Ref.]}}$	$M^{\text{exp}}$ (by ND)	$M^{\text{exp[Ref.]}}$ (by SQUID)	$M^{\text{cal[Ref.]}}$
Co <sub>2</sub> TiGa	Co	0.38	0.40 [20]	0.59 [9]	0.68	0.81 [31]	0.97 [9]
	Ti	−0.08	~0 [20]	−0.19 [9]			
Co <sub>2</sub> VGa	Co	1.04	1.05 [21]	0.95 [18]	2.33	1.95 [18]	1.92 [18]
	V	0.05	~0 [21]	0.05 [18]			
Co <sub>2</sub> CrGa	Co	0.68		0.90 [15]	2.80	3.01 [15]	3.01 [15]
	Cr	1.72 (−0.64)		1.28 [15]			
Co <sub>2</sub> MnGa	Co	0.58	0.52 [22]	0.77 [18]	3.85	4.07 [18]	4.11 [18]
	Mn	2.55 (4.56)	3.01 [22]	2.70 [18]			
Co <sub>2</sub> FeGa	Co	1.28	1.06 [23]	1.19 [15]	5.18	5.17 [15]	5.04 [15]
	Fe	2.77 (0.89)	2.56 [23]	2.76 [15]			

35 K were 0.5781 and 0.5769 nm, respectively. It can be concluded that almost all the atoms are located at the proper sites for the  $L2_1$  phase, being similar to the Co<sub>2</sub>TiGa alloy. From the analysis including magnetic scatterings for the ND pattern taken at 35 K, the magnetic moments of Co and V were evaluated to be about 1.08 and 0.17  $\mu_B/\text{atom}$ , respectively.

### 3.3. Co<sub>2</sub>CrGa

Fig. 5(a) and (b) shows powder ND patterns at 573 and 35 K, corresponding to those in a paramagnetic and a ferromagnetic state, taken from Co<sub>2</sub>CrGa alloy, respectively. Here, while additional small peaks from the second phase appeared at around  $2\theta = 45^\circ$  and  $95^\circ$ , they were excluded from both the ND patterns for the fitting analysis. From the analysis of Fig. 5(b), the values of the  $f_x^{\text{Co}}$  and  $f_z^{\text{Ga}}$  at 35 K were estimated to be 0.98 and 0.88, respectively. This suggests

that although the Co atoms almost perfectly occupy the x site, the Ga and Cr atoms in the y and z sites are comparatively loose. This result accords with the fact that the  $T_{\text{L}2_1/\text{B}2}^{\text{L}2_1/\text{B}2}$  of the Co<sub>2</sub>CrGa alloy is relatively low, as shown in Fig. 1. The magnetic moment of Co is defined to be 0.68  $\mu_B$  and that of Cr on the y and z sites to be 1.78 and −0.64  $\mu_B$ , respectively. In the case of Co<sub>2</sub>CrGa, Co<sub>2</sub>MnGa and Co<sub>2</sub>FeGa alloys, the magnetic moments of Y atoms have a comparatively large value, being contrary to that for the Co<sub>2</sub>TiGa and Co<sub>2</sub>VGa alloys. Thus, we also refined the magnetic moments of Cr, Mn and Fe atoms located on the z site. The magnetic moment of Cr on the y site is larger than theoretical values of 1.14  $\mu_B$  [14] and 1.28  $\mu_B$  [15,16]. As deduced from comparison between the patterns of Figs. 5(a) and (b), the magnetic scattering is very weak and error for the determined values for the magnetic moments might be a little large.

### 3.4. Co<sub>2</sub>MnGa

The ND patterns at 650 and 35 K taken from Co<sub>2</sub>MnGa are shown in Fig. 6(a) and (b), respectively, where a small extra peak appearing at around  $2\theta = 43^\circ$  due to the Mn oxides is excluded. Although the measured temperature  $T_m$  (=650 K) for the pattern of Fig. 6(a) is lower than the  $T_C$  (=685 K), the contribution of the magnetic scattering was neglected in the analysis as well as for the Co<sub>2</sub>VGa. It was estimated that  $f_x^{\text{Co}} = 0.99$  and  $f_z^{\text{Ga}} = 0.94$  for the pattern of 650 K and that  $f_x^{\text{Co}} = 0.98$  and  $f_z^{\text{Ga}} = 0.93$  for that of 35 K, where these sets of the data are consistent with each other. In addition, this result basically accords with the report that a small degree of disorder ( $f_z^{\text{Mn}} = f_y^{\text{Ga}} \approx 0.04$ ) exists [23]. The magnetic moment of Co determined from the pattern of 35 K is 0.58  $\mu_B$ , and Mn on the y and z sites are 2.55 and 4.56  $\mu_B$ , respectively, being comparable to the data reported in previous ND studies [22,23].

### 3.5. Co<sub>2</sub>FeGa

Fig. 7 shows the ND pattern measured at 35 K for the Co<sub>2</sub>FeGa. It is impossible to measure the ND for the specimen with no or very weak spontaneous magnetization because the  $T_C$  (=1093 K) of the Co<sub>2</sub>FeGa [16] is significantly higher than the limitation temperature (650 K) for the measurement in the ND facility. It was found that  $f_x^{\text{Co}} = 0.99$  and  $f_z^{\text{Ga}} = 0.92$ , and that the lattice constant at 35 K is 0.5725 nm. The magnetic moment of Co was estimated to be 1.28  $\mu_B$ , and those of Fe on the y and z sites to be 2.77 and 0.89  $\mu_B$ , respectively.

All the results on the atomic occupancies and the magnetic moments for the Heusler alloys obtained by the present study are listed in Tables 1 and 2. In Table 2, the total magnetic moments experimentally reported by the magnetic measurements with a

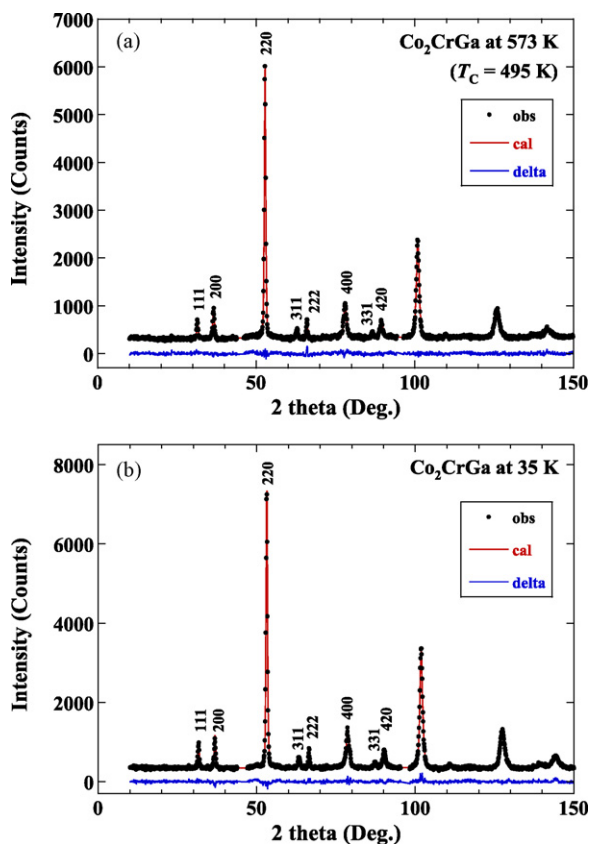


**Fig. 5.** Neutron powder diffraction patterns of Co<sub>2</sub>CrGa alloy measured at 495 K (a) and 35 K (b), displayed in the same way as in Fig. 3.



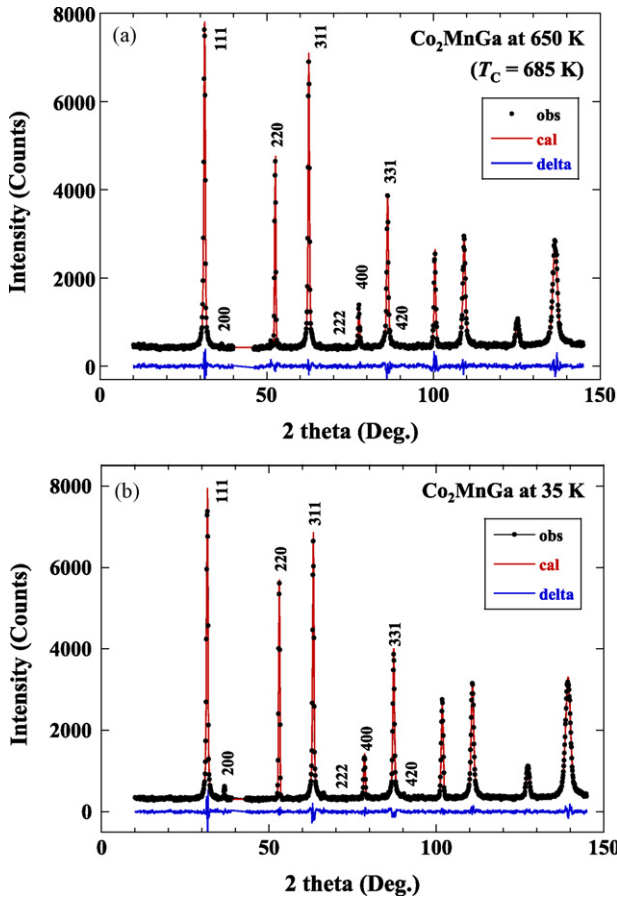


Fig. 6. Neutron powder diffraction patterns of  $\text{Co}_2\text{MnGa}$  alloy measured at 650 K (a) and 35 K (b), displayed in the same way as in Fig. 3.

SQUID magnetometer and theoretically reported with the LMTO-ASA method are also added.

#### 4. Discussion

The site occupancies,  $f_x^{\text{Co}}$  and  $f_z^{\text{Ga}}$ , extracted from the ND patterns of 35 K are plotted in Fig. 8. The  $f_x^{\text{Co}}$  is almost the same in all the alloys, being close to unity, and the Co atoms almost perfectly occupy the x sites. On the contrary, although the  $f_z^{\text{Ga}}$  for  $Y=\text{Ti}$  and  $\text{V}$  are also close to unity, those for  $Y=\text{Cr}$ ,  $\text{Mn}$  and  $\text{Fe}$  are located at around 0.9. As shown in Fig. 1, this behavior is very similar to that of the  $T_t^{L2_1/B2}$  plotted as a function of  $Z_t$ .

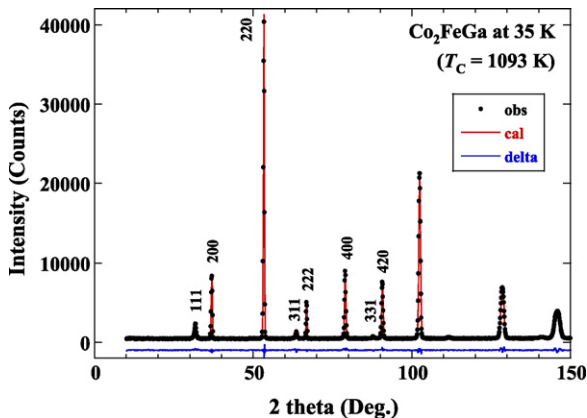


Fig. 7. Neutron powder diffraction pattern of  $\text{Co}_2\text{FeGa}$  alloy measured at 35 K, displayed in the same way as in Fig. 3.

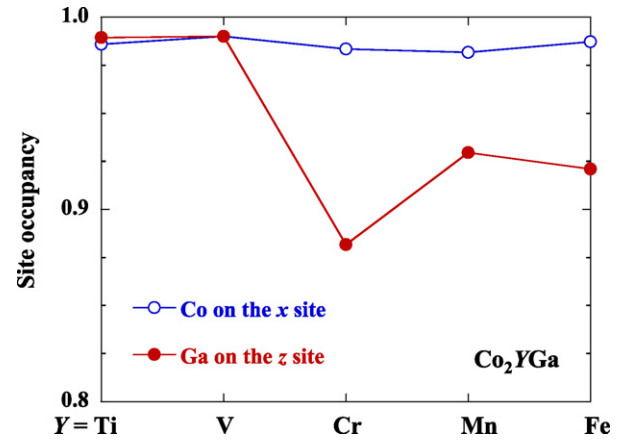


Fig. 8. Site occupancies of the Co and Ga atoms on the x and z sites, respectively, for the  $L2_1$  phase in the  $\text{Co}_2\text{YGa}$  Heusler alloys.

The degree of long-range order in ordered phase depends on temperature and many kinds of thermodynamic approximations to describe the degree of order have been proposed. In the present study, the obtained degree of order for the Heusler alloys was evaluated using Bragg–Williams–Gorsky (BWG) approximation [26–29]. In the BWG approximation [26,27], Gibbs energy is approximately given as the sum of the total bonding energy between the atomic pairs in the  $n$ th nearest neighbor,  $E_n$ , and the configuration entropy term,  $-T\Phi$ , where  $T$  and  $\Phi$  are temperature and configuration entropy, respectively. In the case of the ordered Heusler-phase, one takes into account the bond energies only for  $n \leq 2$ , the free energy,  $F$ , being given by

$$F = E_1 + E_2 - T\Phi. \quad (6)$$

When the pair-wise interchange energies of the  $I$ – $J$  pair in the  $n$ th nearest neighbors are defined as follows using bonding energies of  $I$ – $I$ ,  $J$ – $J$  and  $I$ – $J$  pairs,  $V_{II}^{(n)}$ ,  $V_{JJ}^{(n)}$  and  $V_{IJ}^{(n)}$ :

$$W_{IJ}^{(n)} = \frac{1}{2} \left( V_{II}^{(n)} + V_{JJ}^{(n)} \right) - V_{IJ}^{(n)}, \quad (7)$$

if the  $W_{IJ}^{(2)}$  are neglected, the temperature dependence of the order parameter  $\phi_1$  for the  $B2$ -type phase in the stoichiometric  $X_2YZ$  alloy is simply given by

$$k_B T \ln \frac{(1 + \phi_1)}{(1 - \phi_1)} = 2 \left( 2W_{XY}^{(1)} + 2W_{ZX}^{(1)} - W_{YZ}^{(1)} \right) \phi_1, \quad (8)$$

where  $k_B$  is Boltzmann's constant [29]. In a stoichiometric  $B2$  alloy of the  $X$ – $Y$  binary system,  $W_{ZX}^{(1)}$  can be replaced by  $W_{XY}^{(1)}$  and  $W_{YZ}^{(1)} = 0$  in Eq. (8). Since the relation between the  $W_{XY}^{(1)}$  and the  $B2/A2$  order–disorder transition temperature,  $T_t^{B2/A2}$ , is expressed by  $k_B T_t^{B2/A2} = 4W_{XY}^{(1)}$ , Eq. (8) is modified as follows:

$$\frac{T}{T_t^{B2/L2_1}} = \frac{2\phi_1}{\ln \left( \frac{(1 + \phi_1)}{(1 - \phi_1)} \right)}, \quad (9)$$

which is an expression well-known for binary systems. On the other hand, temperature dependence of the  $\phi_2$  in the stoichiometric  $X_2YZ$  alloy is dependent on the  $\phi_1$  and given [29] by

$$k_B T \ln \frac{(1 + 3\phi_2)}{(1 + 2\phi_1 - 3\phi_2)} = 3W_{YZ}^{(2)}(3\phi_2 - \phi_1). \quad (10)$$

When  $\phi_1 = 1$  is assumed for simplicity, since the  $T_t^{L2_1/B2}$  is given by  $k_B T_t^{L2_1/B2} = 3W_{YZ}^{(2)}$ , Eq. (10) is rewritten as

$$\frac{T}{T_t^{L2_1/B2}} = \frac{(3\phi_2 - 1)}{\ln \left( \frac{(1 + 3\phi_2)}{(3 - 3\phi_2)} \right)}. \quad (11)$$

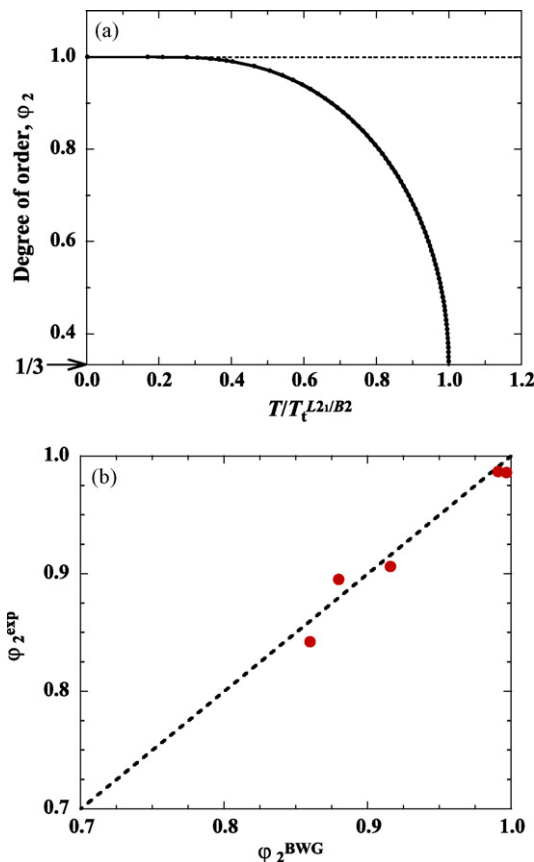


**Fig. 9.** (a) Degree of long-range order  $\phi_2$  for the  $L2_1$  phase calculated using Eq. (11) under an assumption that the Co atoms perfectly occupy the x sites, where the  $\phi_2$  is defined by Eq. (5).  $\phi_2 = 1$  ( $f_z^{\text{Ga}} = 1$ ) means a perfect order state for the  $L2_1$  structure and  $\phi_2 = 1/3$  ( $f_z^{\text{Ga}} = 0.5$ ) the perfect  $B2$  structure expressed with  $\text{Co}_2(\text{Y,Ga})$ . (b) Relation between theoretical and experimental degrees of long-range order,  $\phi_2^{\text{BWG}}$  and  $\phi_2^{\text{exp}}$ , respectively.

Here, Eq. (11) is equivalent to Eq. (9) and the difference in the notation is only due to the definition of order parameters.

Fig. 9(a) shows the  $\phi_2$  calculated by Eq. (11) against the temperature normalized by  $T_{L21/B2}$ . As mentioned above, under the condition  $\phi_1 = 1$ ,  $\phi_2 = 1$  ( $f_z^{\text{Ga}} = 1$ ) means the perfect order state of  $L2_1$  structure, and  $\phi_2 = 1/3$  ( $f_z^{\text{Ga}} = 0.5$ ) is a “perfect”  $B2$  state in which only the Y and Ga atoms randomly occupy the y and z sites. The experimental values of  $\phi_2^{\text{exp}}$  obtained from the  $f_z^{\text{Ga}}$  of 35 K for all the alloys were compared with those calculated by Eq. (11)  $\phi_2^{\text{BWG}}$ , as shown in Fig. 9(b) and listed in Table 1, where for the  $T$  of the experimental data, a final annealing temperature of 773 K was used. Although the experimental order parameters  $\phi_1^{\text{exp}}$  for the Co atoms are not perfect, as shown in Table 1, the values of  $\phi_2^{\text{exp}}$  are in good agreement with the corresponding ones of  $\phi_2^{\text{BWG}}$ . This means that the temperature dependence of the order parameter  $\phi_2$  in the  $\text{Co}_2\text{YGa}$  phase can be predicted using Eq. (11) based on the BWG approximation, if the  $T/T_{L21/B2}$  is known.

## 5. Conclusions

Site occupancies of the Co, Y (Y = Ti, V, Cr, Mn and Fe) and Ga atoms in the  $L2_1$  phase of the  $\text{Co}_2\text{YGa}$  alloys were precisely determined by the powder neutron diffraction measurements. While the Co atoms in all five alloys almost perfectly occupy the x site,

the occupancy of the Ga atoms on the z site depends on the kind of the Y atoms. That is, although being almost perfect in Ti and V alloys, the site occupancy of Ga atoms is around 0.9 in Cr, Mn and Fe alloys. This behavior is consistent with the variation of the order–disorder transition temperature from the  $L2_1$  to the  $B2$  phase of the  $\text{Co}_2\text{YGa}$  alloys. The order parameters of the site occupancy of Ga atoms on z sites experimentally obtained by the ND examinations are in good agreement with the theoretical data evaluated by the Bragg–Williams–Gorsky approximation. This means that for the  $\text{Co}_2\text{YGa}$  Heusler alloys the site occupancy of Ga atoms on z sites at a given temperature can easily be evaluated with the master curve shown in Fig. 9, if the  $T_{L21/B2}$  of the alloy is known.

## Acknowledgements

The present work was supported by a Grant-in-Aid for Scientific Research, from the Japan Society for the Promotion of Science (JSPS) and by Global COE Program “Materials Integration (International Center of Education and Research), Tohoku University,” MEXT, Japan.

## References

- [1] C. Mitra, P. Raychaudhuri, K. Dörr, K.-H. Müller, L. Schultz, P.M. Oppeneer, S. Wirth, Phys. Rev. Lett. 90 (2003) 017202.
- [2] T. Block, C. Felser, G. Jakob, J. Ensling, B. Muhling, P. Gutlich, R.J. Cava, J. Solid State Chem. 176 (2003) 646.
- [3] M. Yamamoto, T. Marukame, T. Ishikawa, K. Matsuda, T. Uemura, M. Arita, J. Phys. D: Appl. Phys. 39 (2006) 824.
- [4] K. Inomata, S. Okamura, A. Miyazaki, M. Kikuchi, N. Tezuka, M. Wojcik, E. Jedryka, J. Phys. D: Appl. Phys. 39 (2006) 816.
- [5] M. Gajek, M. Bibes, S. Fusil, K. Bouzehouane, J. Fontcuberta, A. Barthélémy, A. Fert, Nat. Mater. 6 (2007) 296.
- [6] M.G. Chapline, S.X. Wang, Phys. Rev. B 74 (2006) 014418.
- [7] R.A. de Groot, F.M. Mueller, P.G. van Engen, K.H.J. Buschow, Phys. Rev. Lett. 50 (1983) 2024.
- [8] J. Kübler, A.R. Williams, C.B. Sommers, Phys. Rev. B 28 (1983) 1745.
- [9] S. Ishida, S. Sugimura, S. Fujii, S. Asano, J. Phys. Condens. Matter. 3 (1991) 5793.
- [10] I. Galanakis, P.H. Dederichs, N. Papanikolaou, Phys. Rev. B 66 (2002) 174429.
- [11] C. Felser, G.H. Fecher, B. Balke, Angew. Chem. Int. Ed. 46 (2007) 668.
- [12] Y. Kurtulus, R. Dronskowski, G.D. Samolyuk, V.P. Antropov, Phys. Rev. B 71 (2005) 014425.
- [13] Y. Miura, K. Nagao, M. Shirai, Phys. Rev. B 69 (2004) 144413.
- [14] S. Ishida, S. Kawakami, S. Asano, Mater. Trans. 45 (2004) 1065.
- [15] R.Y. Umetsu, K. Oikawa, K. Kobayashi, R. Kainuma, K. Ishida, N. Endo, A. Fujita, K. Fukamichi, A. Sakuma, Phys. Rev. B 72 (2005) 214412.
- [16] R.Y. Umetsu, K. Kobayashi, R. Kainuma, A. Fujita, K. Fukamichi, K. Ishida, A. Sakuma, Appl. Phys. Lett. 85 (2004) 2011.
- [17] K. Kobayashi, R.Y. Umetsu, R. Kainuma, K. Ishida, T. Oyama, R. Kainuma, K. Ishida, R.Y. Umetsu, A. Fujita, K. Fukamichi, Appl. Phys. Lett. 85 (2004) 4684.
- [18] R.Y. Umetsu, K. Kobayashi, A. Fujita, R. Kainuma, K. Ishida, K. Fukamichi, A. Sakuma, Phys. Rev. B 77 (2008) 104422.
- [19] K. Kobayashi, R.Y. Umetsu, K. Ishikawa, R. Kainuma, K. Ishida, J. Magn. Magn. Mater. 310 (2007) 1794.
- [20] P.J. Webster, K.R.A. Ziebeck, J. Phys. Chem. Solids 34 (1973) 1647.
- [21] K.R.A. Ziebeck, P.J. Webster, J. Phys. Chem. Solids 35 (1974) 1.
- [22] P.J. Webster, J. Phys. Chem. Solids 32 (1971) 1221.
- [23] P.J. Brown, K.U. Neumann, P.J. Webster, K.R.A. Ziebeck, J. Phys.: Condens. Matter. 12 (2000) 1827.
- [24] F. Izumi, T. Ikeda, Mater. Sci. Forum 321–324 (2000) 198.
- [25] K. Kobayashi, R. Kainuma, K. Fukamichi, K. Ishida, J. Alloy Compd. 403 (2005) 161.
- [26] V.S. Gorsky, Z. Phys. 50 (1928) 64.
- [27] W.L. Bragg, E.J. Williams, Proc. R. Soc. A 145 (1934) 699; W.L. Bragg, E.J. Williams, Proc. R. Soc. A 151 (1935) 540.
- [28] S. Matsuda, J. Phys. Soc. Jpn. 8 (1953) 20.
- [29] Y. Murakami, S. Kachi, N. Nakanishi, H. Takehara, Acta Metall. 19 (1971) 97.
- [30] K.H.J. Buschow, P.G. van Engen, J. Magn. Magn. Mater. 25 (1981) 90.
- [31] A. Okubo, R.Y. Umetsu, M. Nagasako, A. Fujita, R. Kainuma, K. Ishida, Scripta Mater. 59 (2008) 830.
- [32] R.Y. Umetsu, A. Okubo, A. Fujita, R. Kainuma, A. Sakuma, K. Ishida, in preparation.